

## Shadow Effects Correction of Aerial Color Image Using Multi-Source Data Sets

Sohn, Hong Gyoo<sup>1)</sup> · Yun, Kong Hyun<sup>2)</sup> · Song, Yeong-Sun<sup>2)</sup> · Park, Hyo-Keun<sup>2)</sup>

<sup>1)</sup> YONSEI University, School of Civil and Environmental Engineering, Professor (sohn1@yonsei.ac.kr)

<sup>2)</sup> YONSEI University, School of Civil and Environmental Engineering, Ph. D. Candidate (ykh1207@yonsei.ac.kr)

<sup>2)</sup> YONSEI University, School of Civil and Environmental Engineering, Ph. D. Candidate (point196@yonsei.ac.kr)

<sup>2)</sup> YONSEI University, School of Civil and Environmental Engineering, Ph. D. Candidate (hkpark@hist.co.kr)

### 요 지

그림자효과 보정은 도심지역에서 영상 해석 또는 지상의 인공지물을 추출하는데 있어서 상당히 중요한 처리과정이다. 본 연구에서는 다중자료원(Multi-Source Data Sets)을 이용하여 컬러항공사진에 발생한 그림자의 효과를 효율적으로 처리 및 보정 할 수 있는 알고리즘을 제시하였으며 시각적인 비교 뿐 만 아니라 도로추출의 시도로 그림자 보정효과의 입증하였다. 또한 다중자료원인 컬러항공사진, LiDAR 고도자료 그리고 1:1000 수치지도를 이용하여 각 센서 및 기존 자료가 가지고 있는 장점을 최대한 살려 시너지 효과를 나타낼 수 있도록 적절한 융합과정을 시도하여 성공적인 예를 보여주었다.

## 1. Introduction

In urban analysis the quality of images can be degraded due to the presence of shadows and occlusions especially in built-up urban areas. The compensation of hidden area can be treated by using multi-view images (Rau et al., 2002). However, due to the characteristic of cast shadow occurrence regardless of sensor position, total correction of shadowed area is not easy. The problem of shadow effects can be solved by modelling shadow regions using multi-source data sets such as Light Detection And Ranging (LiDAR) and an existing digital map. In other words, the modelling of cast shadow is feasible by combing height information obtained from LIDAR data with high height accuracy and feature polygons obtained from an existing digital map which contains positional and attribute data of diverse ground features.

For the correction of shadow effects, it is first necessary to delineate shadow regions from the imagery. Shadow regions can be extracted by using solar position and Digital Surface Model (DSM). Cast shadows, for every pixel of the image, can be determined by tracing a straight line to the solar position over DSM at the time of image acquisition (Giles, 2001). Rau and others (2002) observed that shadow effects could be corrected by the histogram matching method, which is applied to minimize the gray-value differences between a shadow area and its surroundings. The histogram matching methods manipulate the pixel values of one image into the same pixel distribution as another image basically. As a result the shadowed regions are similar to surrounding images in histogram distribution, but the results are not satisfactory in terms of visual inspection.

This study aims at correcting shadow effects from aerial colour imagery using multi-source data sets. For accurate shadow modelling LiDAR data were selected for the generation of DSM. Also, for the accurate correction of shadow effects, segmentation of shadow regions is implemented by using

existing digital map containing surface cover types. The shadow regions are accurately modelled using the solar position obtained from two data sets. Based on our proposed three basic assumptions, the identified shadow regions are replaced into new colour values. Finally, the evaluation of our scheme is made by using region growing methods by comparing the colour imagery before and after the correction of shadow effect.

## 2. The Proposed Scheme

Figure 1 shows the schematic diagram of the proposed method. First, coregistration should be processed between aerial colour image, LIDAR data, and digital map. LIDAR data (WGS84 coordinate) must be transformed into TM coordinate being used in the national coordinate system in Korea, since the three data sets must have the same coordinate system. Due to horizontal error of LIDAR data, it should be coregistered precisely with aerial image or digital map. In this research, the peak points of LIDAR data between building boundary and ground were used for registration. The difference of coordinates between peak points and building boundary of image was calculated and used for horizontal shift of all LIDAR data.

A grid DEM was then produced using elevation contour and spot heights from digital map of 1:1000 scale. Next, the building layer extraction was required from the digital map. A digital map contained many urban related features. Among them, the building polygon was extracted from the digital map. The building was represented as a single polygon in digital map. However, as shown in In figure 2, Aerial color image of study area are shown. For accurate shadow modeling, a polygon representing the rising part of the building was added in the building layer. Therefore, building heights acquired as mean value of LIDAR data within each polygon were entered. Subsequently, shadow regions were delineated through shadow modeling by using solar position, producing DSM.

In the next stage, shadow regions were segmented for accurate shadow effect correction with the help of digital map. Finally, shadow effects were corrected for the segmented shadow region.

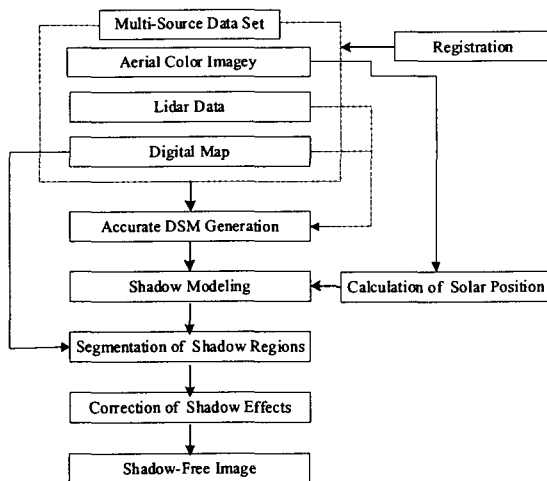


Fig. 1 Schematic diagram of the proposed method.



Fig. 2 Aerial colour image of study area.

## 3. Modelling of Shadow Regions

Modeling of shadow regions serves to calculate shadow length by using height data from LIDAR data, sun elevation angle, and azimuth of aerial image. The shadow length is calculated by

the geometry between building height, elevation angle, and length of shadow. Before modeling of shadow regions, the accurate height value of building must be acquired for the precise correction of shadow effect. The building heights were acquired directly using LIDAR data. LIDAR data within the building polygon had two homogeneous values. One represented the height of the bulk part of building, while the other represented building height except bulk part. However, the building polygon was shown as one polygon in the digital map. To solve this problem, a polygon representing the bulk part of the building was added. Delineation of boundary between bulk part and other part was processed. In other words, one polygon was created by grouping peak points above 1.0 m in comparison with the average of LIDAR data within the polygon. Figures 3 represents the LiDAR data within the building polygon. Figure 4 shows the result of DSM, which is composed of DEM and building height. For the modeling of shadow regions, in addition to building height, solar positions are required at the time of image acquisition. To calculate solar position (sun elevation angle, azimuth), the accurate time, date, latitude, and longitude of study area are needed. The image was acquired on 10 December 2002 around 11:19 am. The longitude of study area was  $127^{\circ} 6' 58''$  while the latitude was  $37^{\circ} 22' 01''$ . If the building height, sun elevation angle and azimuth could be acquired, the modeling of shadows would be possible. solar elevation of  $29.793^{\circ}$  and solar azimuth of  $179.389^{\circ}$  was calculated. For this calculation detail equation are addressed from "NOAA surface Radiation Research Branch" Figure 5 shows the result of shadow modeling using building height, calculated solar elevation and azimuth.

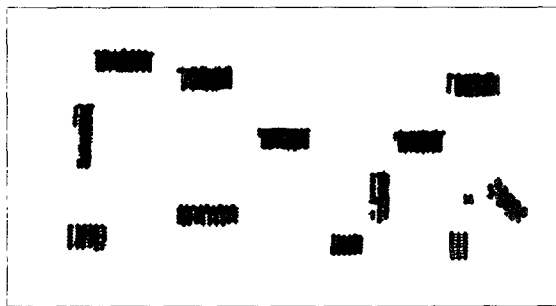


Fig 3. LIDAR data within building polygon

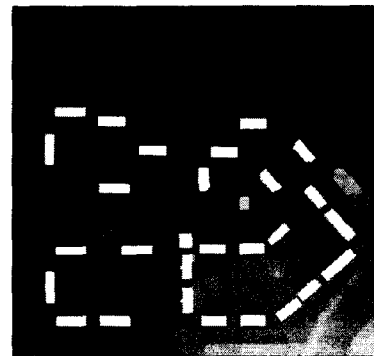


Fig 4. Generation of DSM of the study area

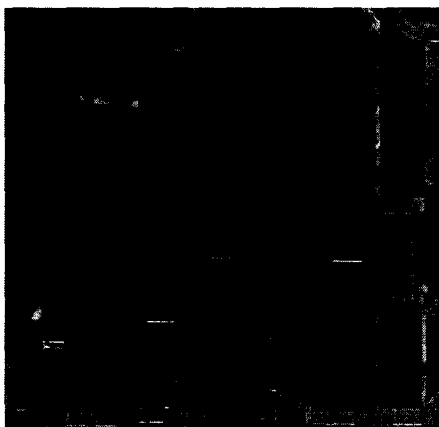


Fig 5. LIDAR data within building polygon

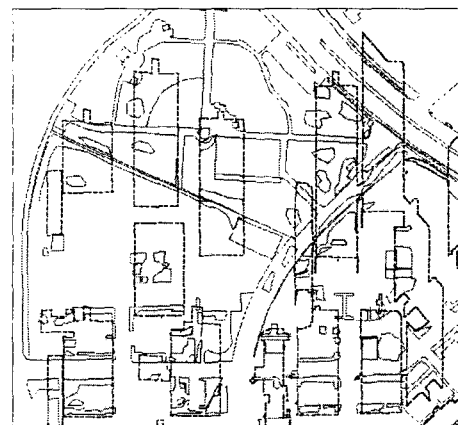


Fig 6. Generation of DSM of the study area

#### **4. Assessment of Shadow Modelling Results**

The proportion of shadow regions in aerial image mainly depends on two factors: the height of buildings on the terrain and the solar elevation angle. Higher buildings and lower solar elevation angle both result in larger shadow regions. Therefore, the accuracy of shadow modelling can vary according to the proportion of shadow region.

To evaluate the accuracy of the shadow modeling algorithm, cast shadows in the corresponding aerial colour image were compared to the output. For this purpose, a volunteer was recruited to independently interpret shadow regions in the aerial image based on the patterns of reduced grey values. This practitioner was experienced in interpreting aerial images, apart from being given instructions for this work. The human interpretation of shadow regions was assumed to be precisely correct. A comparison of the regions marked by the human volunteer to those delineated by the proposed shadow modelling showed that overall accuracy was 97.62%. The proportion of shadow regions in aerial image mainly depends on two factors: the height of buildings on the terrain and the solar elevation angle. Higher buildings and lower solar elevation angle both result in larger shadow regions. Therefore, the accuracy of shadow modelling can vary according to the proportion of shadow region. To evaluate the accuracy of the shadow modeling algorithm, cast shadows in the corresponding aerial colour image were compared to the output. For this purpose, a volunteer was recruited to independently interpret shadow regions in the aerial image based on the patterns of reduced grey values. This practitioner was experienced in interpreting aerial images, apart from being given instructions for this work. The human interpretation of shadow regions was assumed to be precisely correct. A comparison of the regions marked by the human volunteer to those delineated by the proposed shadow modelling showed that overall accuracy was 97.62%.

#### **5. Segmentation of Shadow Regions**

The segmentation of shadows is very important since the results of segmentation have a direct effect on the correction of shadow effects. Shadow regions contain many different surface cover types. Each cover type has a different spectral reflectance. The degree of influence interfered by shadow also varies for each surface type. Therefore, segmentation task is necessary. Polidorio (2003) suggested a technique to segment shaded areas in aerial colour images. This method is based on the physical phenomenon of atmospheric dispersion of sun light, most popularly known as the Rayleigh scattering effect, which is very effective. Because the result showed that shadow regions were not clearly segmented, this method was not relevant. In this study, an existing digital map was utilized for segmentation. By overlapping the extracted shadow region and polygons representing each surface type from digital map, the segmentation task was implemented using intersection operation between two data sets. Fig 6 illustrates the segmentation process.

#### **6. Algorithms for Shadow Effects Correction**

Three basic assumptions to accomplish shadow treatment in aerial image were considered. These were:

- Complete information loss of region hindered by shadow does not occur.
- The influence of cast shadow caused by each object is uniform.
- The DN value of similar surface cover characteristic is uniform.

The first assumption considers that the DN values of shadowed area must not be zero. If the DN values were zero, the recovery of original information would be impossible. In reality, the range of image values of shadow regions is not zero but very low in satellite and aerial images. The second assumption means that the influence of cast shadow caused by blocking of the building must be uniform. Strictly speaking, the influence of shadows near the building is more intensive than that of shadows that are located relatively further from the building. However, the difference is very small. Based on this assumption, only one correction factor could be applicable to radiometric correction for segmented shadow areas. The third assumption explains that the standard deviation of DN values representing one segmented shadow region must be almost zero. If so, the accurate correction of shadow effect could be possible. In reality, one segmented feature of shadow regions in aerial image shows the slight difference of DN values.

Equations (1) and (2) were applied for this study:

$$O^t_{R,G,B}(x,y) = I^t_{R,G,B}(x,y) + \alpha \quad \dots(1)$$

$$\alpha = I^r_{R,G,B}(m) - I^t_{R,G,B}(m) \quad \dots(2)$$

where,  $O^t_{R,G,B}(x,y)$  : DN value of output image at each band.

$I^t_{R,G,B}(x,y)$  : DN value of original image at each band.

$I^r_{R,G,B}(m)$  : mean value of reference area at each band.

$I^t_{R,G,B}(m)$  : mean value of target area at each band.

## 7. Results shadow effect correction

In Figure 7, the corrected image was created using the proposed algorithm. In comparison with the original image, the result showed more enhanced interpretability of aerial colour image. The radiometric correction of asphalt road was very successful. The regions containing diverse and complex ground features showed relatively low correction effect. For example, a parking lot made of paved asphalt included randomly distributed cars, but it was not a unique single polygon in the digital map. Wrong correction of shadow effect occurred accordingly. From the viewpoint of interpretation of urban facilities, its influence could be ignored. Fig 7 shows the corrected image.



Fig 7. Shadow effect corrected image

## 8. Conclusions

In this paper, to enhance the interpretability of aerial colour images, the algorithm correcting shadow effects by combining digital map and LIDAR data in image was described and experimented. In the process of shadow region delineation, the shadow modelling is implemented using LIDAR data and solar position. In comparison to manual extraction, 97.62 percent of the cast shadow pixels are detected using the high vertical accuracy of LIDAR data.

In the part of shadow effects correction, some conventional correction algorithms have significant drawbacks in that detailed atmospheric data are required and the process is complex. In contrast, a simpler correction method shows insufficient accuracy. The proposed algorithms here are comparatively simple by using the relationship between similar land surface types (similar or same surface types in shadow and in shadow-free area), but it shows excellent correction results. Also, shadow region segmentation using an existing digital map in built-up urban areas can enable us to perform correction with high accuracy. In the stage of evaluation of shadow effect correction, the correction algorithms are proved as successful partially.

This researches show how to make a wise choice among a possible data that are available for urban areas, and illustrate how to fuse multi source data sets to achieve a given purpose using extracted information from individual data.

## References

- Giles, P.T. 2001. Remote Sensing and Cast Shadows in Mountainous Terrain. *Photogrammetric Engineering and Remote Sensing*, 67(7):833-839.
- Polidorio, A.M, F. C. Flores, N. N. Imai, A .M. G. Tommaselli, and C. Fransco. 2003. Automatic shadow segmentation in aerial colour images. *Proceeding of the XVI Brazilian symposium on computer graphics and image processing*, 270-277.
- Rau, J.Y., N.Y., Chen, and L.C. Chen. 2002. True orthophoto generation of built-up areas using multi-view images. *Photogrammetric Engineering and Remote Sensing*, 68(6):581-588.